Barium Titanate-Enhanced Hexagonal Boron Nitride inks for Printable High-Performance Dielectrics

Hyunho Kim[1], Adrees Arbab[1], Benji Fenech-Salerno[1], Chengning Yao[1], Ryan Macpherson[1] Jong Min Kim[2] and Felice Torrisi[1]

[1] Molecular Sciences Research Hub, Department of Chemistry, Imperial College London, White City Campus, 82 Wood Lane, London W12 0BZ, United Kingdom

[2] Department of Engineering, University of Cambridge, 9 JJ Thompson Avenue, Cambridge CB3 0FA, United Kingdom

E-mail: f.torrisi@imperial.ac.uk

Received xxxxxx
Accepted for publication xxxxxx
Published xxxxxx

Abstract

Printed electronics have been attracting significant interest for their potential to enable flexible and wearable electronic applications. Together with printable semiconductors, solution processed dielectric inks are key in enabling low-power and high-performance printed electronics. In the quest for suitable dielectrics inks, two-dimensional materials such as hexagonal boron nitride (h-BN) have emerged in the form of printable dielectrics. In this work, we report barium titanate ($BaTiO_3$) nanoparticles as an effective additive for inkjet-printable h-BN inks. The resulting inkjet printed h-BN/$BaTiO_3$ thin films reach a dielectric constant (ε_r) of ~ 16 by adding 10% of $BaTiO_3$ nanoparticles (in their volume fraction to the exfoliated h-BN flakes) in water-based inks. This result enabled all-inkjet printed flexible capacitors with C ~ 10.39 nF cm^{-2}, paving the way to future low power, printed and flexible electronics.

Keywords: dielectric, printed electronics, hexagonal boron nitride, barium titanate nanoparticle

1. Introduction

Printed electronics has the potential to enable low-power, large scale flexible electronics.[1] Low operation voltages (< 5V), thin films (< 10 μm) and solution processable materials are key to achieve high-performance printed and flexible electronic components.[2, 3] Active electronic devices are normally composed of a semiconductor, a conductor, and a dielectric material.

While a lot of effort has been placed in the development of solution processed semiconductors with high mobility and on/off current ratio, printable dielectric inks are relatively less investigated. Thin films of printed nanomaterials often suffer from existing pinholes which results in relatively low breakdown strengths (B_v) of < 1 MV m^{-1}. Organic dielectrics can offer higher B_v but lower dielectric constant (ε_r). It is challenging to achieve high performance printed electronics, and these limit the establishment of all printed electronic components such as field-effect transistors (FETs) and energy storage devices.

Printable dielectrics have been developed by using cross-liked polymer blends such as poly(4-vinyl)phonol and silane reagents, achieving ε_r ~ 5.7 and B_v ~ 3-6 MV cm^{-1}.[4]

Recently, nanomaterials have been used in the form of additives or conductive filler to improve the dielectric properties. Gold nanoparticles have been grafted with thiol-terminated polystyrene, resulting in printed dielectric films achieving $\varepsilon_r \sim 50$ and $B_v \sim 39.1$ MV m^{-1}.[5] On the other hand, high ε_r nanoparticles such as barium titanate ($BaTiO_3$) can be considered for higher dielectric performance. For example, nanocomposite of $BaTiO_3$ and poly(vinylidene fluoride-co-hexafluoro propylene) dielectric thin films show $\varepsilon_r \sim 20$ and $B_v \sim 260$ MV m^{-1}.[6] $BaTiO_3$ is one of the most used dielectric material with a high ε_r of around 500 at room temperature.[7] This is due to their perovskite structure where a central Ti atom can make a large displacement under external electric field. $BaTiO_3$ is one of the key materials in the application of multi-layer ceramic capacitors (MLCC),[8] while their use as gate dielectric is much less studied in detail.

Inks based on two-dimensional (2D) materials have been demonstrated to be a suitable platform for printed electronics[9], with the charge transport dominated by the inter-flake or intra-flake hopping.[10] Large scale production of 2D materials by liquid-phase exfoliation (LPE),[11] microfluidic exfoliation,[12] or electrochemical exfoliation (EE)[13] yields electronic few-layer 2D material inks, with conducting (e.g., MXenes)[14], semiconducting (e.g., transition metal dichalcogenides)[15, 16], and insulating properties (e.g., hexagonal boron nitride (h-BN) or silicates)[17] suitable for printed and flexible electronics on-demand and in scale.[18]. h-BN consists of a lattice of boron and nitrogen atoms arranged in a honeycomb structure.[19] Single layer h-BN flakes have a wide band gap of ~ 6.47 eV, which is larger than their bulk counterpart (5.95 eV).[20] The out-of-plane ε_r of h-BN is 3.29 and 3.76 for monolayer and bulk, respectively, which is comparable to that of SiO_2 (3.8).[21] Moreover, inorganic h-BN offers a better chemical stability against oxygen, moisture, and heat than organic dielectrics.[22] Inkjet printable dielectric inks with few-layer h-BN (FL h-BN) flakes and carboxymethylcellulose (CMC) resulted in ε_r of ~ 7 and $B_v \sim 1$ MV m^{-1},[17] which falls in a similar range of polymer printable dielectrics.

However, printed dielectric films still suffer from a low B_v and the associated high leakage current, mostly due to the presence of pinholes and defects in the film. In addition, a manufacturing issue related to the roughness of these printed inks, contributes to regions of high electric field density in the dielectric the leading to breakdown. Another limitation reported, especially with the use of high boiling point solvents is the required annealing during printing or post-processing for solvent removal, which poses severe limitations when printing on plastic or textile substrates.[23, 24]

In this work we demonstrate water-based h-BN inkjet printable dielectric ink with $\varepsilon_r \sim 16$, formulated by using 10% (in volume fraction to the exfoliated h-BN flakes) of $BaTiO_3$ nanoparticles as an additive, and show its viability for all-inkjet printed flexible capacitors with a capacitance of 10.39 nF cm^{-2}.

2. Experimental

2.1 Sample Preparation

2.1.1 Hexagonal boron nitride (h-BN) ink formulation. 3 g of carboxymethyl cellulose sodium salt (CMC) (weight-average molecular weight, M_w = 700,000, Sigma Aldrich, no. 419338) was added to 1 liter (1000 mL) of deionized water and was placed on a magnetic stirring plate overnight. Once the CMC was fully dissolved, 4 g of h-BN powder (Goodfellows B516011, <10 μm size) (concentration ~ 4mg mL^{-1}) was added to the solution and stirred until the solution become homogenized. The mixture was then microfluidized (M110-P Microfluidizer by Microfluidics) at a pressure of 200 MPa for 50 cycles. The h-BN ink was then centrifuged at 3000 rpm using a Thermo Fisher Scientific ultracentrifuge using a TH-641 swinging rotor for 20 minutes. The supernatant was carefully collected for further study.

2.1.2 Barium titanate ($BaTiO_3$) ink formulation. 3 mg mL^{-1} of CMC was added to deionized water and allowed to dissolve overnight with the aid of a magnetic stirrer. Once the CMC was dissolved, 10 mg mL^{-1} of $BaTiO_3$ nanopowder (cubic crystalline phase) (Sigma Aldrich, no. 467634) was added to the water CMC mixture and then sonicated for 9 hrs (Fisherbrand FB15069, Max power 800 W). The BaTiO3 ink was then centrifuged (Thermo Fisher Scientific ultracentrifuge using a TH-641 swinging) at 1000 rpm for 20 minutes. The supernatant was carefully collected for further study.

2.1.3 Hybrid h-BN and $BaTiO_3$ dielectric ink formulation. h-BN and $BaTiO_3$ inks were mixed in a volume ratio of 9:1 to form a hybrid h-BN/$BaTiO_3$ dielectric ink. Once the h-BN and $BaTiO_3$ inks were mixed in the appropriate ratio, the mixture was sonicated for a period of 5 minutes allowing a homogeneous h-BN/$BaTiO_3$ ink to form.

2.1.4 Device architecture. Metal insulator metal (MIM) capacitor structures were used to characterize the dielectric ink. These are comprised of three different layers which were fabricated on a Polyethylene terephthalate (PET) substrate. The first layer was made of a sliver (Ag) film (Novacentrix JS-AS102A) with a dimension of 2.25 mm x 2.25 mm, this was followed by a dielectric layer which has 1.50 mm x 1.50 mm dimension. Finally, the top layer was a Ag electrode of 0.5 mm x 0.5 mm in size.

2.2.5 Inkjet printing. A drop on demand (DoD) Fujifilm Dimatix DMP-2800 mounting a Fujifilm DMC-11610 cartridge (nozzle diameter ~ 21 µm) was used ink jet printing system, producing individual droplets with a volume of ~ 10 pL. The platen temperature was switched off during the printing process and the cleaning cycle was set at 60 s. The Z number ($Z = \frac{1}{Oh} = \frac{\sqrt{\rho\gamma a}}{\eta}$) is the inverse of the Ohnesorge number (Oh) which is defined as $Oh = \frac{\eta}{\sqrt{\rho\gamma a}}$ where γ is surface tension (mN m^{-1}), ρ is density (g cm^{-3}), a is diameter of inkjet nozzle (μm), and η is viscosity (mPa s). Ideally, inks suitable for inkjet printing need to have Z between 1 and 24. [17, 18] The inter-drop distance is the space between two adjacent droplets that was measured from the center of each drop after deposition. A uniform printed film is formed when the inter-drop distance is smaller than the drop diameter, and a uniform printed layer is formed as the drops merge without coalescing. The inter-drop distance for the bottom and top sliver (Ag) electrodes in the MIM were 30 µm, whereas the dielectric material was printed with an inter-drop distance of 10 µm. Each Ag electrode was fabricated via 2 printing passes while the printing passes for the dielectric material was varied. MIM devices were made from dielectric inks which had 6, 8 and 10 printing passes. Three sets of MIM devices were made from h-BN, $BaTiO_3$ and hybrid h-BN/$BaTiO_3$.

2.1.6 Capacitance measurement. The capacitance of MIM capacitors is measured by a precision impedance analyzer (Agilent 4294) connected to probe station (Cascade Microtech Summit 12000). An equivalent series resistor-capacitor circuit was used to extract capacitance from impedance measurement.[25] The impedance amplitude is given by $|Z| = \sqrt{R^2 + (\omega C)^{-2}}$ where R is series resistance, ω is angular frequency, and C is capacitance. The areal capacitance was calculated by dividing the capacitance (at 100 kHz) by the area of top electrode. The dielectric constant (ε_r) is calculated by $\varepsilon_r = Ct/\varepsilon_0 A$ where t is thickness of dielectric layer, ε0 is dielectric permittivity of free space, and A is top electrode area.

3. Results and Discussions

3.1 h-BN ink

Figure 1(a) shows an SEM image (inset) and the statistics of the lateral sizes of obtained h-BN flakes. The log normal distribution is peaked at ~ 345 nm, which is in the same order of magnitude of printable h-BN inks previously reported.[17] The average particle size results ~ 60 times smaller than the nozzle diameter (a = 21 µm) of our printing cartridge, thus avoiding nozzle clogging. The morphology of h-BN flakes are shown in the inset SEM image. **Figure 1(b)** plots the UV-vis absorption spectra of FL h-BN ink with a peak centered at 208 nm (inset), which corresponds to intrinsic inter-band transition,[26] revealing an optical band gap, E_g of ~ 5.96 eV. The Raman spectrum of h-BN ink deposited on glass substrate is shown in **Figure 1(c)** revealing a single peak at 1366 cm^{-1} attributed to E_{2g} phonon vibrations, indicating that our h-BN flakes are few layers (3-5) thick.[27] **Figure 1(d)** shows the X-ray diffraction (XRD) curves of the h-BN ink (FL h-BN) deposited on glass substrate compared to bulk h-BN powder. The absence of non-basal plane peaks such as (100), (101), and (102) suggests excellent degree of exfoliation and restacking structure of h-BN flakes perpendicular to substrate normal.[28, 29] The h-BN flakes were characterized by AFM (**Figure S1**), where the lognormal distribution of flake's thickness was found to be ~ 6 nm.

3.2 $BaTiO_3$ ink

Figure 2(a) shows the statistics of the size distribution of $BaTiO_3$ nanoparticles with the log-normal distribution peaked at 243 nm. The SEM image in the inset shows the morphology of $BaTiO_3$ nanoparticles that is printed from diluted ink. The UV-vis absorption spectrum of the $BaTiO_3$ ink is shown in **Figure 2(b)**. Smooth absorption edge is found which agree with literature,[30] and the inset Tauc plot, extrapolation of linear onset of $(\alpha h\nu)^2$ verses $h\nu$ plot, reveals optical band gap of ~ 3.0 eV. The estimated optical band gap is slightly smaller than that of bulk $BaTiO_3$ (3.2 eV), which can be attributed to band gap narrowing in nanoparticles and strain.[31] It is worth noting that the absorption coefficients of $BaTiO_3$ nanoparticles are found to be 536.57 L g^{-1} m^{-1} and 241.39 L g^{-1} m^{-1} for the wavelengths of 660 and 1000 nm, respectively. In order to optimize the $BaTiO_3$ nanoparticle dispersion, different ultrasonication times were investigated for an initial concentration (c_i) of ~ 10 mg mL^{-1}. As shown in **Figure 2(c)**, sonication time of at least 9 hours (followed by a centrifugation at 1000 rpm) is required to achieve a higher c ~ 3.52 mg mL^{-1}, while shorter sonication times did not produce such high concentration. The longer sonication time was not effective to increase concentration further. **Figure 2(d)** shows XRD spectra of printed $BaTiO_3$ thin film. The $BaTiO_3$ nanoparticle are in high crystallinity despite of their small particle size. The inset shows detailed spectra for (200) peak without distinct peak splitting, which confirms the cubic phase instead of tetragonal. The (200) peak center is found to be 2θ = 45.19° by fitting to Pseudo-Voigt function.

3.3 hybrid h-BN/$BaTiO_3$ ink

We investigate the evolution of the the ε_r of the pure h-BN inks as a function of $BaTiO_3$ nanoparticles introduced in the dispersion. However, keeping the majority of dielectric material in the ink in the form of flakes with a large aspect ratio allows to maximise the stacking of the dispersed

elements, while reducing the film thickness and the suraface roughness in printed $BaTiO_3$/h-BN thin films. A rough surface may cause non uniform dielectric performances and pin-holes or difficulty in printing as a function of multiple printing passes. Also, a highly rough surface may result in very hydrophobic profile even though the nanosheet iteself is hydrophilic, hindering drop coalescence and eventually preventing the formation of a uniform dielectric film.[32] For these reasons in addition to h-BN and $BaTiO_3$ inks, we prepared an $BaTiO_3$/h-BN ink by blending h-BN and $BaTiO_3$ inks so that to keep h-BN flakes and $BaTiO_3$ nanoparticles in a 9:1 ratio. **Figure 3(a)** summarizes and compares the characteristics of three inks in terms of concentration (c), viscosity (η) and Z parameters.

In order to determine the printability of prepared inks, we first analysed the Z parameter which gives an indication of the jettability of a given ink from a nozzle (see methods). We determine the following rheological parameters: $\gamma_{\text{h-BN}}$ ~ 73.76 mN m^{-1}, $\rho_{\text{h-BN}}$ ~1.004 g cm^{-3}, $\eta_{\text{h-BN}}$ ~ 1.94 mPa·s; γ_{BTO} ~ 73.88 mN m^{-1}, ρ_{BTO} ~1.007 g cm^{-3}, η_{BTO} ~ 4.78 mPa·s; $\gamma_{\text{h-BN/BTO}}$ ~ 73.77 mN m^{-1}, $\rho_{\text{h-BN/BTO}}$ ~1.005 g cm^{-3}, $\eta_{\text{h-BN/BTO}}$ ~ 2.22 mPa s. Similar values were found for γ and ρ of the different inks, due to the dominant 3 mg mL^{-1} CMC in water as stabilizer. The Z parameters of h-BN, $BaTiO_3$, and 10% $BaTiO_3$/h-BN are 20.32, 8.25, and 17.73 respectively. The Ohnesorge number can be further divided into Weber number (We) and Reynolds number (Re): $Oh = (We)^{1/2}/Re$, $Re = V\rho a/\eta$, and $We = V^2\rho a/\gamma$, where V is flow speed that is assumed as 6 m s^{-1}.[33] **Figure 3(b) and 3(c)** show the relationship between *Re* and *Oh*, and between *Oh* and *We*, respectively, showing that all three inks fits into the printable fluid regime. We draw the horizontal line for $1 < Z < 24$ that is defined as the optimal range for printing.[17, 18] Previous studies have discussed possible satellite droplets might occourred at $Z > 10$,[34, 35] we could notice such behavior in the case of h-BN ink (Z=20.32) but not in the 10% $BaTiO_3$/h-BN ink (Z=17.73). (**Figure 3(d)**)

All three inks meet the Z parameter requirement for successful printing. A small addition of $BaTiO_3$ ink into the h-BN ink resulted in a great modulation in the viscosity and Z parameter. The $BaTiO_3$/h-BN ink contains 1.01 mg mL^{-1} of h-BN and 0.35 mg mL^{-1} of $BaTiO_3$. Considering the density of nanomaterials (2.1 g cm^{-3} for h-BN, and 6.02 g cm^{-3} for $BaTiO_3$), the relative mass fraction of $BaTiO_3$ 34.6% corresponds to an equivalent volumatric fraction of 10.7%.

3.4 Inkjet-printed MIM capacitors

We have fabricated MIM capacitors to evaluate the dielectric performance of inkjet-printed thin films. **Figure 4(a)** shows the schematic cross-section of an all-printed MIM capacitor using silver and dielectric inks. **Figure 4(b)** shows the optical microscopy images of printed MIM devices. The dark squares correspond to the silver electrodes and white squares to the dielectric film. **Figure 4(c)** shows the areal capacitance (see methods) of h-BN and 10% $BaTiO_3$/h-BN as a function of number of printing passes for the dielectric film. A larger value of printing passes corresponds to a larger thickness of the dielectric thin film. Each printing passes increase the thickness of the printed thin film approximately 270 nm. (**Figure S2**) The MIM capacitors with 10% $BaTiO_3$/h-BN dielectric layer have clearly higher areal capacitance than the ones with pure a h-BN dielectric layer. The former ranging from a 4.5 nF cm^{-2} for 10 printing passes to 10 nF cm^{-2} for 6 printing passes, while the latter ranging from 3.2 nF cm^{-2} to 4.5 nF cm^{-2} for 6 printing passes. This represents clear evidence that the 10% $BaTiO_3$ nanoparticle additive effectively boosts the dielectric performance of printed h-BN film. As a result, the ε_r of h-BN thin film of 10.1 has increased to 16 after embedding $BaTiO_3$ nanoparticles while keeping the inkjet printability (**Figure 4(d)**). The breakdown voltages of the 10% $BaTiO_3$/h-BN capacitors with printing passes of 4, 6, and 8 are found to be 6.1V, 14.9 V, and 32.6 V, respectively. The equivalent breakdown strengths are 6.3 MV/m, 9.2 MV/m, and 14.6 MV/m. The leakage current remained at the level of few hundreds nA/mm^2. (**Figure S3**)

The achieved enhancement of εr can be considered by Landauer's effective medium approximation (EMA) with below equation.[36]

$$x_1 \frac{(\rho_1 - \rho_m)}{(\rho_1 + 2\rho_m)} + x_2 \frac{(\rho_2 - \rho_m)}{(\rho_2 + 2\rho_m)} = 0$$

where x_1 and x_2 are volumetric fraction of individual materials, ρ_1 and ρ_2 are material's property, and ρ_m is the approximated property of the mixture material. We can apply material 1 and 2 as h-BN/CMC and $BaTiO_3$/CMC, respectively, where $x_1 = 0.9$, $x_2 = 0.1$, $\rho_1 = 10.11$, and $\rho_2 = 430.81$. By using quadratic formula for ρ_m, the effective solution for the dielectric constant of the mixture is calculated as 13.94 which is slightly smaller than the measured value of 16. This suggests that there could have been additional synergic effect occurred once the h-BN/$BaTiO_3$ film is formed. For example, the small gaps between the $BaTiO_3$ nanoparticles could have been filled by smaller FL h-BN.

4. Conclusions

We report an inkjet-printable water-based h-BN dielectric ink achieving a dielectric constant (ε_r) of 16. A 10% addition of $BaTiO_3$ nanoparticle to the dispersion results in an improvement of the dielectric constant of more than 50% on the pure h-BN ink. This result demonstrates that the hybrid combination of dielectric 2D materials and nanomaterials is a powerful route for the development of high-*k* printable dielectrics.

Acknowledgements

The authors acknowledge funding from EPSRC grants EP/P02534X/2, EP/R511547/1, EP/T005106/1, the Imperial College Collaboration Kick-Starter grant.

ORCID iDs

Hyunho Kim: https://orcid.org/0000-0003-2381-9716
Benji Fenech-Salerno: https://orcid.org/0000-0002-0150-9672
Chengning Yao: https://orcid.org/0000-0001-5446-8088
Felice Torrisi: https://orcid.org/0000-0002-6144-2916

References

[1] Khan Y, Thielens A, Muin S, Ting J, Baumbauer C and Arias A C 2020 *Adv. Mater.* **32** 1905279
[2] Matsui H, Takeda Y and Tokito S 2019 *Org. Electron.* **75** 105432
[3] Torrisi F and Carey T 2018 *Nano Today* **23** 73-96
[4] Kim C, Wang Z M, Choi H J, Ha Y G, Facchetti A and Marks T J 2008 *J. Am. Chem. Soc.* **130** 6867-78
[5] Buchheit R, Kuttich B, Gonzalez-Garcia L and Kraus T 2021 *Adv. Mater.* **33** 2103087
[6] Yang K, Huang X Y, Huang Y H, Xie L Y and Jiang P K 2013 *Chem. Mater.* **25** 2327-38
[7] Petrovsky V, Petrovsky T, Kamlapurkar S and Dogan F 2008 *J. Am. Ceram. Soc.* **91** 3590-2
[8] Zhang Y C, Wang X H, Kim J Y, Tian Z B, Fang J, Hur K H and Li L T 2012 *J. Am. Ceram. Soc.* **95** 1628-33
[9] Torrisi F and Coleman J N 2014 *Nat Nanotechnol* **9** 738-9
[10] Piatti E, Arbab A, Galanti F, Carey T, Anzi L, Spurling D, Roy A, Zhussupbekova A, Patel K A, Kim J M, Daghero D, Sordan R, Nicolosi V, Gonnelli R S and Torrisi F 2021 *Nat. Electron.* **4** 893-905
[11] Hernandez Y, Nicolosi V, Lotya M, Blighe F M, Sun Z Y, De S, McGovern I T, Holland B, Byrne M, Gun'ko Y K, Boland J J, Niraj P, Duesberg G, Krishnamurthy S, Goodhue R, Hutchison J, Scardaci V, Ferrari A C and Coleman J N 2008 *Nat Nanotechnol* **3** 563-8
[12] Karagiannidis P G, Hodge S A, Lombardi L, Tomarchio F, Decorde N, Milana S, Goykhman I, Su Y, Mesite S V, Johnstone D N, Leary R K, Midgley P A, Pugno N M, Torrisi F and Ferrari A C 2017 *ACS Nano* **11** 2742-55
[13] Su C Y, Lu A Y, Xu Y P, Chen F R, Khlobystov A N and Li L J 2011 *ACS Nano* **5** 2332-9
[14] Zhang C F, McKeon L, Kremer M P, Park S H, Ronan O, Seral-Ascaso A, Barwich S, Coileain C O, McEvoy N, Nerl H C, Anasori B, Coleman J N, Gogotsi Y and Nicolosi V 2019 *Nat. Commun.* **10** 1795
[15] Kelly A G, Hallam T, Backes C, Harvey A, Esmaeily A S, Godwin I, Coelho J, Nicolosi V, Lauth J, Kulkarni A, Kinge S, Siebbeles L D A, Duesberg G S and Coleman J N 2017 *Science* **356** 69-72
[16] Carey T, Arbab A, Anzi L, Bristow H, Hui F, Bohm S, Wyatt-Moon G, Flewitt A, Wadsworth A, Gasparini N, Kim J M, Lanza M, McCulloch I, Sordan R and Torrisi F 2021 *Adv. Electron. Mater.* **7** 2100112
[17] Carey T, Cacovich S, Divitini G, Ren J S, Mansouri A, Kim J M, Wang C X, Ducati C, Sordan R and Torrisi F 2017 *Nat. Commun.* **8** 1202
[18] Torrisi F, Hasan T, Wu W P, Sun Z P, Lombardo A, Kulmala T S, Hsieh G W, Jung S J, Bonaccorso F, Paul P J, Chu D P and Ferrari A C 2012 *ACS Nano* **6** 2992-3006
[19] Golberg D, Bando Y, Huang Y, Terao T, Mitome M, Tang C C and Zhi C Y 2010 *ACS Nano* **4** 2979-93
[20] Wickramaratne D, Weston L and Van de Walle C G 2018 *J. Phys. Chem. C* **122** 25524-9
[21] Laturia A, Van de Put M L and Vandenberghe W G 2018 *Npj 2d Mater Appl* **2** 6
[22] Brebels J, Manca J V, Lutsen L, Vanderzande D and Maes W 2017 *J. Mater. Chem. A* **5** 24037-50
[23] Ren J S, Wang C X, Zhang X, Carey T, Chen K L, Yin Y J and Torrisi F 2017 *Carbon* **111** 622-30
[24] Ji X Q, Liu W W, Yin Y J, Wang C X and Torrisi F 2020 *J. Mater. Chem. C* **8** 15788-94
[25] Kelly A G, Finn D, Harvey A, Hallam T and Coleman J N 2016 *Appl. Phys. Lett.* **109** 023107
[26] Hoffman D M, Doll G L and Eklund P C 1984 *Phys. Rev. B* **30** 6051-6
[27] Gorbachev R V, Riaz I, Nair R R, Jalil R, Britnell L, Belle B D, Hill E W, Novoselov K S, Watanabe K, Taniguchi T, Geim A K and Blake P 2011 *Small* **7** 465-8
[28] Li L H, Chen Y, Behan G, Zhang H Z, Petravic M and Glushenkov A M 2011 *J. Mater. Chem.* **21** 11862-6
[29] Li L H, Chen Y, Cheng B M, Lin M Y, Chou S L and Peng Y C 2012 *Appl. Phys. Lett.* **100** 261108
[30] Khan M A M, Kumar S, Ahamed M, Ahmed J, Kumar A and Shar M A 2021 *J Mater Sci-Mater El* **32** 12911-21
[31] Ramakanth S and Raju K C J 2014 *J. Appl. Phys.* **115** 173507
[32] Zhao M Q, Xie X Q, Ren C E, Makaryan T, Anasori B, Wang G X and Gogotsi Y 2017 *Adv. Mater.* **29** 1702410
[33] Chuang M Y, "Inkjet Printing of Ag Nanoparticles using Dimatix Inkjet Printer, No 2", Protocols and Reports. Paper 40. and http://repository.upenn.edu/scn_protocols/40
[34] Derby B 2011 *J. Eur. Ceram. Soc.* **31** 2543-50
[35] Maleki H and Bertola V 2020 *Catal Sci Technol* **10** 3140-59
[36] Landauer R 1952 *J. Appl. Phys.* **23** 779

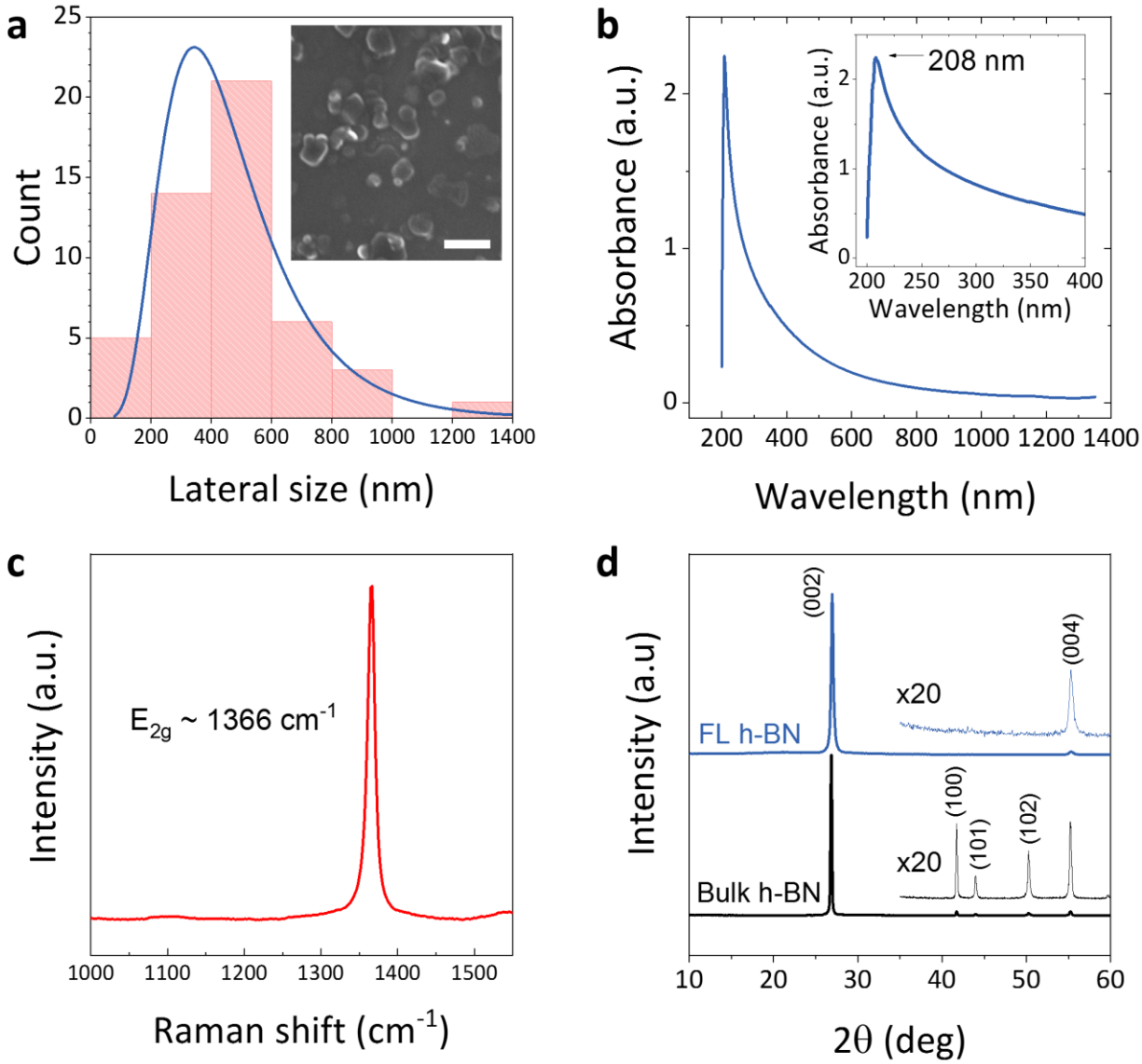

Figure 1. Characterization of h-BN dispersion in aqueous solution of 3 mg mL^{-1} CMC. **a)** Lateral size distribution of h-BN flakes. Inset is SEM image of h-BN printed by diluted ink. Scale bar is 1 µm. **b)** UV-vis absorption spectra of h-BN ink. Inset is shorter range plot near absorbance maxima. **c)** Raman spectra of printed h-BN thin film. **d)** XRD pattern of printed h-BN thin film and bulk powder.

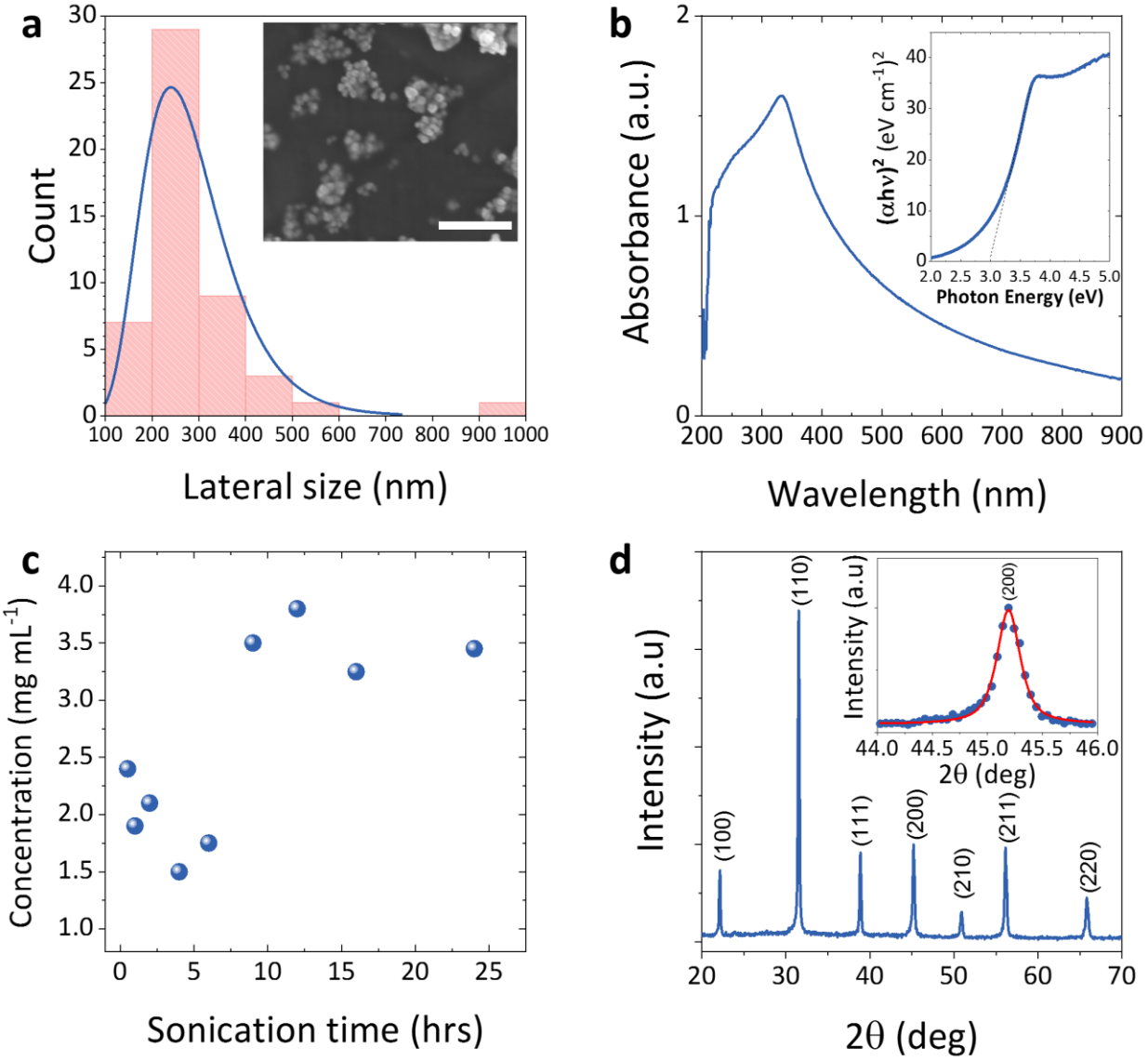

Figure 2. Characterization of $BaTiO_3$ nanoparticle dispersion in aqueous solution of 3 mg mL^{-1} CMC. **a)** Lateral size distribution of $BaTiO_3$ nanoparticle. Inset is SEM image of $BaTiO_3$ printed by diluted ink. Scale bar is 1 μm. **b)** UV-vis absorption spectra of $BaTiO_3$ ink. Inset is corresponding Tauc plot, revealing optical band gap of 3.0 eV. **c)** Concentration of $BaTiO_3$ inks as a function of ultrasonication time. Initial concentration is 10 mg mL^{-1}. **d)** XRD pattern of printed $BaTiO_3$ film. Inset shows detailed (200) peak with Pseudo-Voigt fitting.

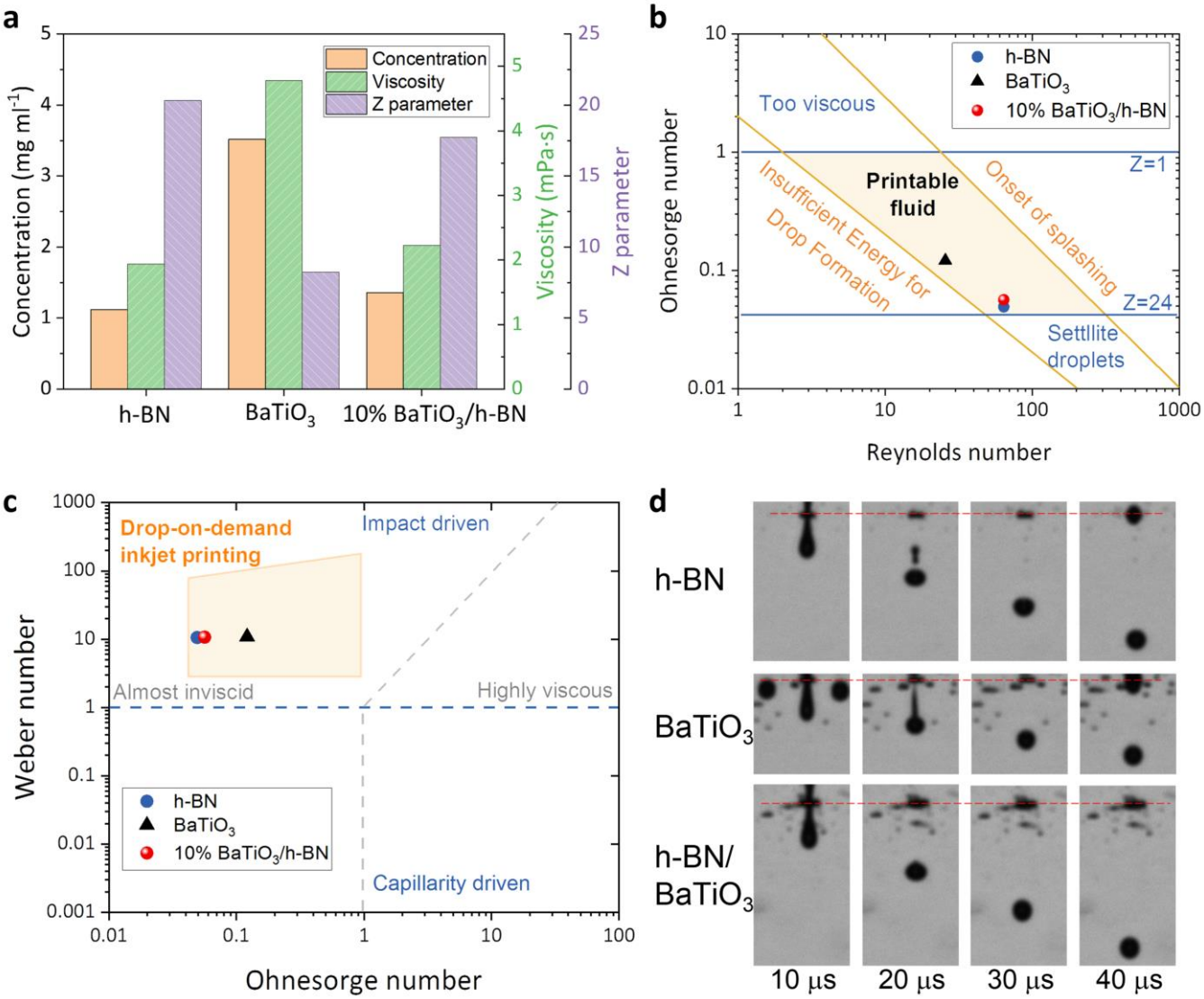

Figure 3. Comparison of h-BN, $BaTiO_3$, and 10% $BaTiO_3$/h-BN inks. **a)** Concentration, infinite rate viscosity, and Z parameter plots. **b-c)** Parameter mapping of **(b)** Reynolds and Ohnesorge numbers, and **(c)** Ohnesorge and Weber numbers of prepared inks in 3 mg mL^{-1} CMC in water. (**d)** Optical microscopy images of inkjet-printed droplets for h-BN ink (Z=20.32), $BaTiO_3$ ink (Z=8.25), and 10% $BaTiO_3$/h-BN ink (Z=17.73). Images were taken after jetting with the chosen delay. (Each row consists of 4 different droplets) Red dashed lines indicate the position of nozzle. The droplet volume is 10 pL. The area above the red dashed line shows the reflection of droplets.

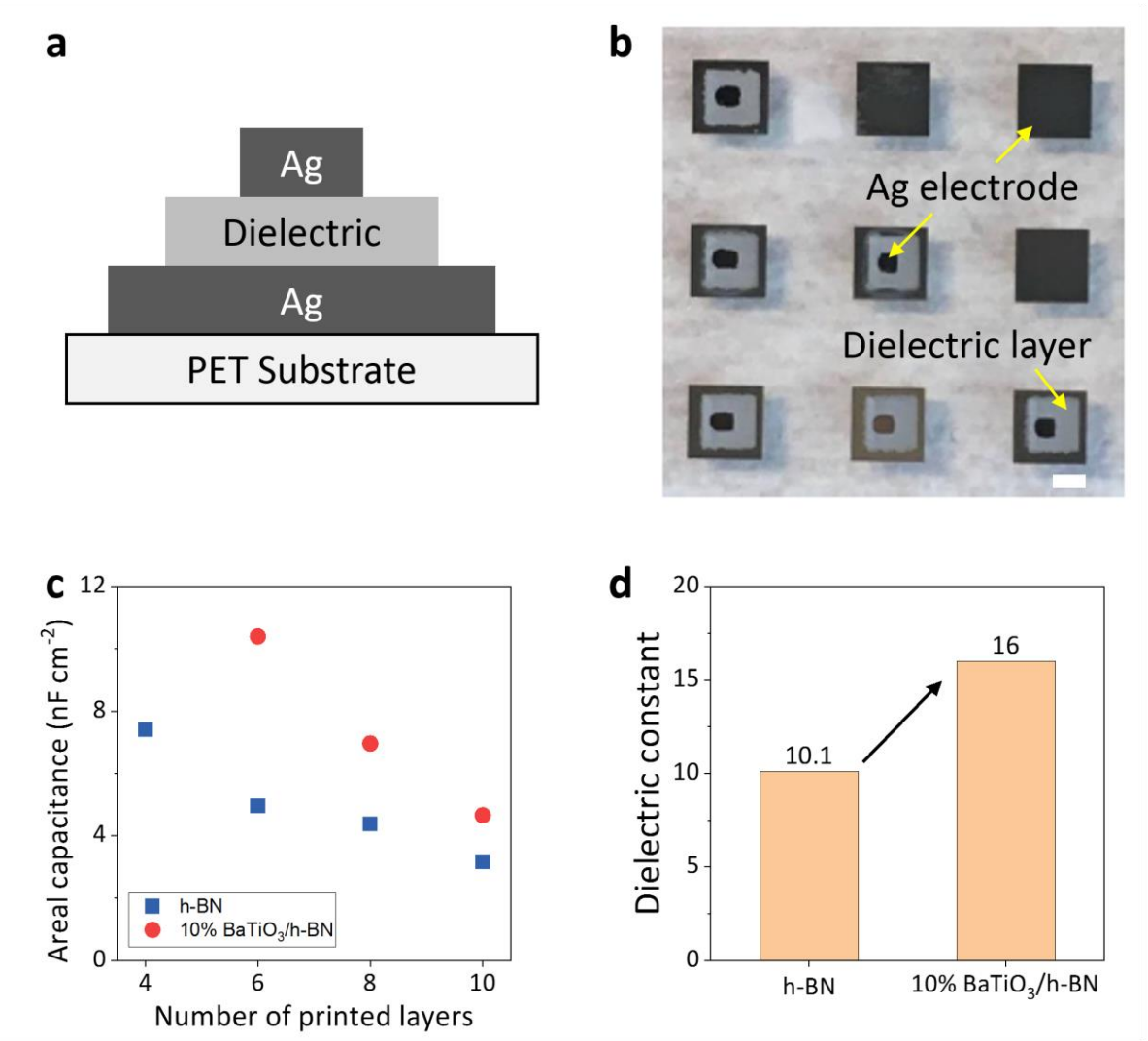

Figure 4. a) Schematic sideview illustration of printed MIM capacitor. **b)** Optical microscope images of MIM capacitor array. Arrows denote the top and bottom Ag electrode, and dielectric layer between the Ag electrodes. Scale bar is 1mm. **c)** Areal capacitance of dielectric layers as a function of number of printed layers. **d)** Dielectric constants of h-BN thin films with and without 10% $BaTiO_3$ nanoparticles.